Nearly Equidistant Single Swift Heavy Ion Impact Sites Through Nanoporous Alumina Masks.

Xavier Cauchy and Sjoerd Roorda

Département de Physique, Université de Montréal, C.P. 6128, Succursale Centre-Ville, Montréal, Québec, Canada H3C 3J7

Abstract. A semi-ordered pattern of 70 MeV Ag single ion impact sites on a fused silica sample was achieved by irradiation through a free-standing 10 μm through-pore ordered nanoporous alumina membrane. The membranes were fabricated by constant voltage anodization in oxalic acid with a two-step replication process. An apparatus and a method were developed to realize the alignment of the pores parallel to the ion beam. Measurements of the surface, by atomic force microscopy, confirm the presence of a semi-ordered pattern of single ion impact sites.

Keywords: Mask, Swift Heavy Ion, Single Impact, Nanoporosity..
PACS: 78.67.Rb, 79.20.Rf, 61.85.+p

INTRODUCTION

The modification of materials by swift heavy ion beams has attracted considerable attention since the discovery of ion tracks in the midst of the last century [1, 2, 3, 4]. These latent tracks find applications such as nanopore filters [5], cold emitters [6], and ultrasmall transistors [7]. Although nowadays the use of ion beams is common in the making of devices such as semiconductor transistors, the random nature of single ion impacts considerably complicates its usage in nanomodeling. Here, we show that it is possible to obtain ordered arrays of single impact sites of swift heavy ions by exposing the sample through a nanoporous alumina mask. The self-organizing ability of porous anodic alumina was first discovered by Masuda and Fukuda [8]. Since then, Masuda and Satoh described a two-step technique to replicate the long range pore organization to initial pore formation [9] and thereby obtain a highly parallel array of pores of typical interpore distance 100 nm on a hexagonal lattice. Using different electrolytes and voltages, Li et al. [10] obtained organized arrays of interpore distance 50 - 420 nm. Nanoporous anodic alumina since then served as a template for ion lithography [11], for nanodot formation [6] and for nanowire formation [12]. However, single equidistant ion impacts were never observed to our knowledge. We start from the method described by Masuda and Satoh to obtain 9 - 10 μm thick nanoporous alumina membranes, as revealed by SEM micrographs A simple yet effective

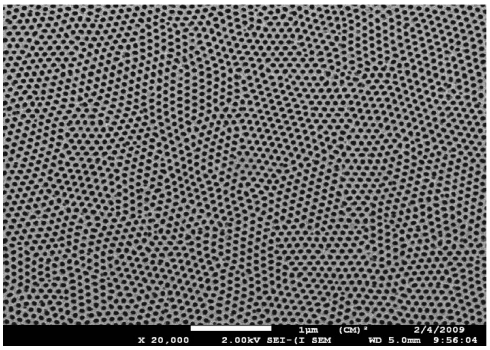

FIGURE 1A. Field-effect scanning electron microscopy image of the front surface of an alumina mask. The picture shows small domains of a self-organized 2-D hexagonal lattice.

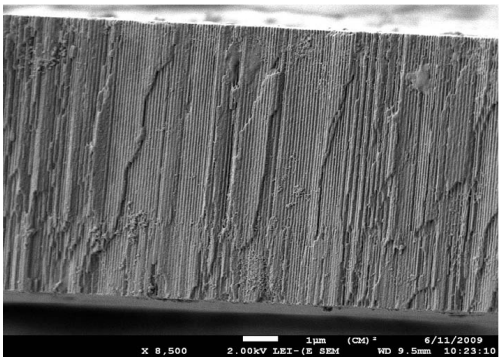

FIGURE 1B. A cross section of an alumina mask (a mask was sacrificed and broken in two in order to take this picture). Notice the pores are straight over their entire length of more than 8 μm.

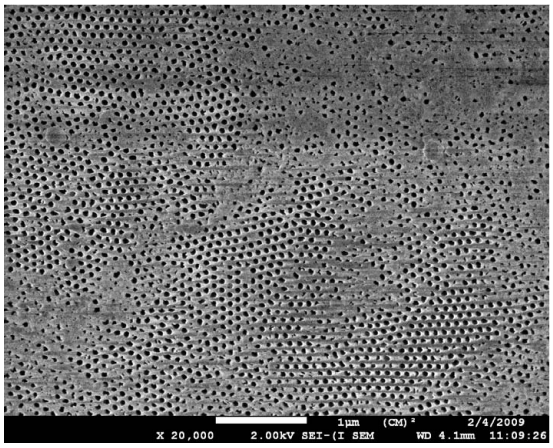

FIGURE 1C. Back side (bottom) of an alumina mask. Most pores are completely open, a small amount of material remains to obscure the remaining pores.

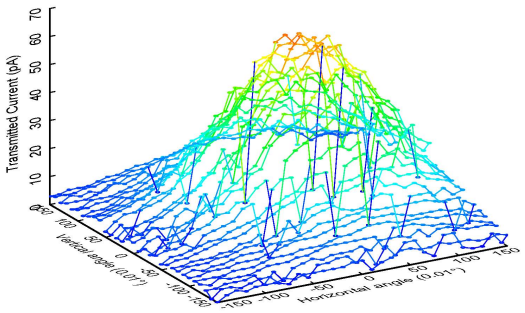

FIGURE 2. Ion current measured in transmission for 1.5 MeV Li ions through a nanopore mask as a function of vertical and horizontal angle between the mask's surface normal and the incident ion beam. Maximum deflection is 1.5º in either direction.

method is developed to dissolve the pore's barrier layers. The samples are aligned by positioning the sample in a 1.5 MeV Li beam so the transmitted current is at its maximum. The beam is then switched to a 70 MeV Ag beam and fused silica is bombarded through the mask. The resulting impact pattern is investigated by atomic force microscopy (AFM). Pore ordering is partially preserved in isolated ion impact positions.

Figures 1 (a), (b), and (c) show the top, side, and bottom view of a prepared mask, as seen in a field-effect scanning electron microscope. The three characteristics crucial for our application are (1) the presence of domains of pores arranged in a well-ordered hexagonal lattice, (2) the straightness of the pores so that ions can channel through them unencumbered, and (3) most pores have opened and those that have not are only covered by a thin layer through which the high energy ions are easily transmitted.

Figure 2 presents the raw data of the ion current recorded on the Faraday cup versus the angle between the alumina mask's normal direction and the beam direction for the motion given by the two motors. A 1.5 MeV Li ion beam was used, and the angle was varied between -1.5º and +1.5º in steps of 0.1º. Clearly a maximum transmission occurs when the surface normal of the mask is oriented close to the ion beam direction. A quantitative analysis shows that the transmission data can be described by gaussian fits with a width of $\sigma = (0.64 \pm 0.02)^\circ$ in the horizontal and $(0.69 \pm 0.02)^\circ$ in the vertical direction. The reason for the shape of the transmission profile is attributable to multiple parameters such as ion range, beam angular dispersion, sample surface oscillations and pore obstructions slightly deviating the beam. It is clear however that there is a narrow range which we can call the aligned position. Once the sample is correctly positioned, it is left untouched and the beam is changed to 70 MeV Ag ions. The distance between the last focusing element and the sample is ≈ 8 m, which insures a negligible change in the beam direction. We have tested the alignment in consecutive Li beam setups leaving the goniometer untouched and it was found to be perfectly aligned even after completely resetting the accelerator.

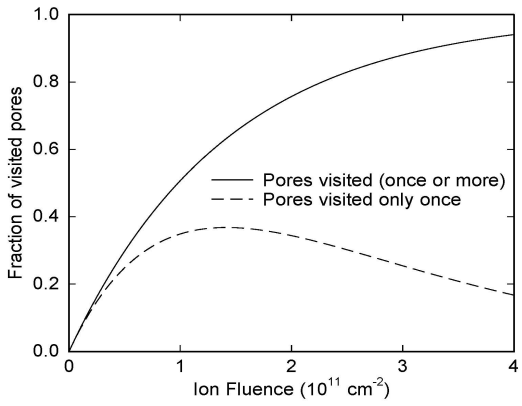

FIGURE 3. Calculated probability of one or more ions passing through a pore (solid line) or exactly one, and not more than one, ion passing through a pore (dashed line) as a function of ion fluence incident at normal angle on a nanopore mask. The effective pore diameter was taken as 30 nm and the pore density as 114 pores/μm^2.

The required implantation fluence for an optimal number of single impact sites is calculated using a simple computer simulation determining what proportion of pores were visited overall and what proportion represents pores visited only once. Figure 3 gives the evolution with fluence of these two quantities. A maximum in the number of single impacts is reached when the proportion of pores visited reaches 60-70 %. The implantation was planned with a target proportion of 70 % of pores visited and was performed using a sample of fused silica under the mask.

RESULTS AND DISCUSSION

Fused silica is known to display hillocks after high velocity ion impacts [13, 14] or depressions after low velocity impacts [6]. We can therefore observe directly the impact sites with AFM on the surface of the fused silica sample.

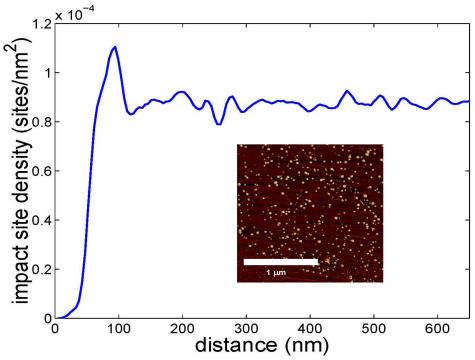

FIGURE 4. Pair distribution function of impact sites as measured by AFM. Distances less than 50 nm between impact sites are strongly avoided. Inset: Phase shift atomic force microscopy (AFM) image of a silica sample after irradiation with 70 MeV Ag ions through a nanopore mask. The bright dots correspond to hillocks and indicate single in impact sites.

The inset of Figure 4 presents a phase shift AFM image of the surface of a sample bombarded with our setting. The topology image confirmed that the features observed were hillocks, which is consistent with swift heavy ions impacts. To the naked eye, the pattern appears less disordered than the pattern for a non-masked irradiation to a similar fluence, but one cannot clearly distinguish the hexagonal lattice so obviously visible in the SEM images of the pore arrangement itself (see Figure 1). In order to determine if some of the pore pattern was transferred to the sample, we determined the radial probability distribution function of impacts, where each impact is replaced by a dot and a threshold is set under which we ignore the features on the image to eliminate natural oscillations and noise. A mild smoothing is applied by convoluting the PDF obtained with a hexagonal function.

The curve in Figure 4 is the result of our routine applied to the image presented as an inset. It is clear from this result that close proximity (<50 nm) impact sites are inhibited. Also, the peak at 100 nm is consistent with the spacing of the pores on the mask used, so it strongly suggests that impact sites are preferably aligned with the mask's pores. Moreover, we see that at long range, the impact density converges to a value of $\approx 0.85 \times 10^{-4}$ impacts per nm^2 which is coherent with the predicted value of 0.81×10^{-4} impacts per nm^2 corresponding to 0.7 times the mask pore density, which confirms that the ions that hit the membrane were either stopped or slowed down enough so that there were no hillocks created on the fused silica. This is strong evidence that it is possible to induce order in swift heavy ion impact sites using nanoporous alumina membranes as an implantation mask.

Small changes in the mask fabrication process could yield far better results. One of the first problems to address would be the surface undulations of the alumina membrane. Whatever care is taken in their handling, pure aluminum sheets always display macroscopic range undulations in their surface, meaning the statistics on the directions of the pores formed must show a relatively high standard mean deviation. This makes impossible a perfect alignment over the sample surface. Therefore, a rigid and perfectly flat substrate should be used for aluminum which could undergo chemical etching and would survive electropolishing and anodizing steps.

CONCLUSION

In summary, it has been shown that it is possible to align a thick (9-10 µm) nanoporous alumina membrane parrallel to ion beam. It has also been shown that the alumina can be used as an implantation mask for swift heavy ions. Finally, we have obtained a nearly equidistant pattern of swift heavy ion impact sites on fused silica showing a clear peak at 100 nm on the PDF by using nanoporous alumina as an implantation mask.

EXPERIMENTAL METHODS: MASK FABRICATION

Aluminum samples of high purity (99.999 %) were cut to 2.5 by 4 cm pieces and straightened. The samples were then ultrasonically cleaned in acetone and ethanol and rinsed in distilled water. Research shows [15, 10] that better pore ordering is obtained after annealing of the aluminum. Samples are therefore annealed at 400 °C for 4 hours under vacuum. Electropolishing is then performed in a 1:3 mix of perchloric acid and methanol, respectively, kept under 20 °C in an ice bath. A 15 V potential with a current density of 0.4 A/cm^2 for 2-3 minutes yielded the best results. Before the first anodization step, the rough side of the aluminum sample is covered with Chemtronics Konform SR Silicone Coating to inhibit oxide formation on one side.

The first anodization is performed in a 0.3 M oxalic acid bath at 5 °C under a constant voltage of 40 V for 4 hours. After this step the pores are assumed to have reached their equilibrium position. The oxide layer is then dissolved in a solution of chromic and phosphoric acids of respective concentrations 0.2 and 0.3 M at boiling point for 1 hour. Removing the bottom of the pores leaves a pattern of valleys and ridges on the bare aluminum surface, the valleys corresponding to the pore's equilibrium positions. The anodization is then repeated under the same conditions for 3 hours. The pores initiate in the valleys and are therefore initially in their equilibrium position.

Although one surface was covered with isolating coating, a small amount of oxide grows underneath the isolating layer. A window is delicately scratched on the backside of the sample with a diamond point pen corresponding to the size of the alumina window we wish to obtain. The bare aluminum on this area is then selectively dissolved in a mixture of saturated copper sulfate and hydrochloric acid as described by Ding et al. [16], thus avoiding the use of toxic mercury chloride. This method has the advantage of leaving a frame of aluminum untouched outside of the desired area which facilitates the handling of the alumina membrane.

The intended use of the membranes being of selectively blocking or channeling incoming swift heavy ions, we wish the ion path inside of the pore to be completely free. Anodic alumina membranes inherently show a barrier layer at the bottom of the pores which we wish to remove. We then prepare a 5% phosphoric acid solution and place one drop of this solution directly on the backside of the alumina membrane where the pores are closed. A wiper placed under the sample starts to wet when the acid comes through the sample, meaning some pores were opened. We then immerse the complete membrane in the solution for 5 more minutes for further pore opening. We then rinse the sample thoroughly in distilled water.

The sample to be exposed is mounted on a two axis goniometer and the alumina mask is placed directly on top of the sample in such a way that only half the membrane covers the sample. The goniometer was fabricated for our purpose and consists of an aluminum plate mounted on three contact points. Two of those contact points are Squiggle linear motors which can move normal to the aluminum plate surface. The small diplacement of one contact point is then equivalent to a rotation around an axis determined by the two other contact points. The goniometer has a hole corresponding to the intersection with the beam path. When mounted correctly, the part of the mask not covering the sample coincides with this hole so that ions passing through the mask are free to be collected on a faraday cup at the end of the line. We use a 1.5 MeV Li beam generated by a 6 MV tandem accelerator with the goniometer placed in the implantation chamber for the alignment of the sample. We seek a maximum in the current collected on the faraday cup. Following irradiation the samples were imaged with a Digital Instruments Nanoscope AFM in tapping mode with a scan rate 2.5 Hz.

ACKNOWLEDGMENTS

We gratefully acknowledge the expert assistance of Louis Godbout with the operation of the Tandem accelerator. This work was financially supported by NSERC and FQRNT.

REFERENCES

1. D.A. Young. The discovery of solid-state nuclear tracks–a personal memoir from 1956-1959, *Radiation Measurements* **44** (2009) 704–706..
2. L. T. Chadderton and H. M. Montagu-Pollock. Fission Fragment Damage to Crystal Lattices : Heat-Sensitive Crystals. *Royal Society of London Proceedings Series A*, **274**:239–252, July 1963.
3. J. J. Kelsch, O. F. Kammerer, A. N. Goland and P. A. Buhl. Observation of fission fragment damage in thin films of metals. *Journal of Applied Physics*, **33(4)**:1475–1482, 1962.
4. R. L. Fleischer, P. B. Price, R. M. Walker and E. L. Hubbard. Track registration in various solid-state nuclear track detectors. *Phys. Rev.,* **133(5A)**:A1443– A1449, Mar 1964.

5. C. Daubresse, T. Sergent-Engelen, E. Ferain, Y.-J. Schneider, and R. Legras, *Nucl .Instr. Meth. B*. **105** (1995) 126 , and: E. Ferain and R. Legras, *Nucl .Instr. Meth. B*. **174** (2001) 116.
6. T.E. Felter, R.G. Musket, and A.F. Bernhardt, *Nucl. Instr. and Meth*. *B* **241** (2005) 346–350
7. J. Chen, R. Könenkamp, *Appl. Phys. Lett*., **82** 4782 (2003)
8. H. Masuda and K. Fukuda. Ordered metal nanoholes arrays made by a two-step replication of honeycomb structures of anodic alumina. *Science*, **268**(5216): 1466–1468, Jun 1995.
9. H. Masuda and M. Satoh. Fabrication of gold nanodot array using anodic porous alumina as an evaporation mask. *Jap. J. of Appl. Phys. Pt. 2, Letters*, **35(1)**:L126–L129, 1996.
10. A. P. Li, F. Műller, A. Birner, K. Nielsch and U. Gősele. Hexagonal pore arrays with a 50–420 nm interpore distance formed by self-organization in anodic alumina. *Journal of Applied Physics,* **84(11)**:6023–6026, 1998.
11. A. Razpet, A. Johansson, G. Possnert, M. Skupinski, K. Hjort, and A. Hallén, *J. Appl. Phys*. **97**, 044310 (2005).
12 S. Takami, Y. Shirai, T. Chikyow, and Y. Wakayama, *Thin Sol. Films* **518**, 692 (2009).
13. A.M.J.F. Carvalho, A.D. Touboul, M. Marinoni, C. Guasch, M. Ramonda, H. Lebius, F. Saigné and J. Bonnet. Single swift heavy ion-induced trail of discontinuous nanostructures on SiO2 surface under grazing incidence. *Thin Solid Films*, **517(1)**:289 – 292, 2008.
14. I. H. Wilson, J. B. Xu, R. A. B. Devine and R. P. Webb. Energetic ion impacts on quartz surfaces : a study by atomic force microscopy. *Nucl. Instr. and Meth. B*, **118(1-4)**:473 – 477, 1996.
15. Jinsub Choi. *Fabrication of Monodomain Porous Alumina using Nanoimprint Lithography and its Applications.* Thesis, Mathematisch-Natturwissenschaftlich-Technischen Fakultaet (Ingenieurwissenschaftlicher Bereich) der Martin-Luther-Universitaet Halle-Wittenberg, Halle, Allemagne, Septembre 2003.
16. GQ Ding, MJ Zheng, WL Xu and WZ Shen. Fabrication of controllable freestanding ultrathin porous alumina membranes. *Nanotechnology*, **16(8)**:1285– 1289, AUG 2005.